44th AIAA Aerospace Sciences Meeting and Exhibit
9 - 12 January 2006, Reno, Nevada

AIAA-2006-1517

Breakup of Turbulent and Non-Turbulent Liquid jets in Gaseous Crossflows

Khaled A. Sallam,[*] Chee-Loon Ng[†] and Ramprakash Sankarakrishnan[‡]
Oklahoma State University, Stillwater, Oklahoma, 74078-5016

and

Christian Aalburg[§] and Kyungjin Lee[**]
The University of Michigan, Ann Arbor, Michigan, 48109-2140

An experimental and computational investigation of the primary breakup of nonturbulent and turbulent round liquid jets in gas crossflow is described. Pulsed shadowgraph and holograph observations of jet primary breakup regimes, conditions for the onset of breakup, properties of waves observed along the liquid surface, drop size and velocity properties resulting from breakup and conditions required for the breakup of the liquid column as a whole, were obtained for air crossflows at normal temperature and pressure. The test range included crossflow Weber numbers of 0-2000, liquid/gas momentum ratios of 100-8000, liquid/gas density ratios of 683-1021, Ohnesorge numbers of 0.003-0.12, jet Reynolds numbers of 300-300,000. The results suggest qualitative similarities between the primary breakup of nonturbulent round liquid jets in crossflows and the secondary breakup of drops subjected to shock wave disturbances with relatively little effect of the liquid/gas momentum ratio on breakup properties over the present test range. The breakup of turbulent liquid jets was influenced by a new dimensionless number in terms of liquid/gas momentum ratio and the jet Weber number. Effects of liquid viscosity were small for present observations where Ohnesorge numbers were less than 0.4. Phenomenological analyses were successful for helping to interpret and correlate the measurements.

Nomenclature

d_i	=	*streamwise jet diameter at onset of drop formation*
d_j	=	*liquid jet diameter at jet exit*
d_{li}	=	*diameter of ligaments at liquid jet surface*
d_p	=	*diameter of drops formed by primary breakup*
Oh	=	*Ohnesorge number,* $\mu_L/(\rho_L d_j \sigma)^{1/2}$
q	=	*flow momentum ratio,* $\rho_L v_j^2/(\rho_G u_\infty^2)$
Re	=	*Cross stream Reynolds number,* $\rho_G u_\infty d_j/\mu_G$
Re_{Ld}	=	*liquid jet Reynolds number,* $\rho_L V_j d_j/\mu_L$

[*] Assistant Professor, School of Mechanical and Aerospace Engineering, 218 Engineering North, Member AIAA. Corresponding author, Tel.: +1-405-762-0749; Fax: +1-405-744-7873; E-mail address: khaled.sallam@okstate.edu.
[†] Graduate Student Research Assistant, School of Mechanical and Aerospace Engineering, Student Member AIAA.
[‡] Graduate Student Research Assistant, School of Mechanical and Aerospace Engineering.
[§] Research Fellow, Department of Aerospace Engineering, Member AIAA.
[**] Research Fellow, Department of Aerospace Engineering, Member AIAA.

SMD = *Sauter mean diamenter*
t = *time*
t^* = *characteristic time,* $d_j(\rho_L/\rho_G)^{1/2}/u_\infty$
u = *crosstream velocity*
v = *streamwise velocity*
We = *crossflow Weber number,* $\rho_G d_j u_\infty^2/\sigma$
$We_{L\Lambda}$ = *jet Weber number,* $\rho_L \Lambda V_j^2/\sigma$
x = *crosstream distance*
y = *streamwise distance*
λ_c = *wavelength for liquid column waves*
λ_s = *wavelength for liquid surface waves*
μ = *molecular viscosity*
Λ = *Radial (cross stream) turbulent integral length scale*
ν = *molecular kinematic viscosity*
ρ = *density*
σ = *surface tension*

Subscripts
b = *location of breakup of entire liquid jet*
Bag = *bag property*
G = *gas property*
i = *location of onset of breakup*
j = *jet exit property*
l = *ligament property*
L = *liquid property*
p = *property of drops formed by primary breakup*
∞ = *ambient gas property*

I. Introduction

The present research program on the breakup of liquid jets in gas crossflows was conducted by Prof. Faeth and motivated by applications of spray breakup in crossflow to air-breathing propulsion systems, liquid rocket engines, diesel engines, spark ignition engines, and agricultural sprays, among others. This paper will review the findings of Faeth group[1-4] at the University of Michigan as well as new research findings at Oklahoma State University. Earlier studies of nonturbulent round liquid jets in gas crossflows were recently reviewed by Wu et al.[5]; therefore, the discussion of early work will be brief. Initial research on nonturbulent round liquid jets in gas crossflows mainly concentrated on the penetration lengths and the jet/spray plume trajectories for various flow conditions.[6-17] The primary breakup properties of liquid jets in crossflow have recently received more attention, however, with Wu et al.[5] reporting similarities between the primary breakup properties of round liquid jets in gas crossflows and the secondary breakup properties of drops subjected to shock wave disturbances. Wu et al.[5] observed bag, multimode and shear breakup regimes along the liquid column. They also identified conditions required for the breakup of the entire liquid column itself and the trajectory properties of the liquid jet.

The objectives of this research program were to extend the studies of Wu et al.[5] by observing the properties of uniform nonturbulent round liquid jets in uniform gas crossflows, seeking to quantify effects of parameters known to influence breakup regimes transitions and properties of primary breakup along the liquid surface, and to provide information about the drop properties resulting from gas crossflows acting on round nonturbulent liquid jets. The objectives were also to investigate the effects of liquid turbulence on the breakup properties. Present observations included pulsed shadowgraph and holographs of nonturbulent and turbulent round liquid jets of various liquids (water, ethyl alcohol, and a glycerol mixture) in air crossflows at normal temperature and pressure. The shadowgraph and holograms were used for flow visualization and to provide new measurements about jet primary breakup regimes transitions, conditions for the onset of breakup along the liquid surface, the properties of liquid surface waves along the liquid surface, the properties of ligaments and drops due to primary breakup, the properties of drop velocities after primary breakup, and finally the properties of breakup of the entire liquid column as a whole. Finally, The objectives of the computational study was to develop a computational method to study the properties of sprays at the small liquid/gas density ratios and large Ohnesorge number conditions of interest for practical high pressure combustion processes.

II. Experimental Methods

The experiments were carried out in a rectangular shock tube with the driven section having a width of 38 mm and a height of 64 mm. The driven section was open to the atmosphere and had windowed side walls in order to provide optical access as shown in Fig. 1. The shock tube provided test times of 17-21 ms in the uniform flow region behind the shock wave. Crossflow velocities of 11-142 m/s were considered, which involved nearly normal temperature and pressure conditions in the crossflow. The experiments were also carried out in a subsonic wind tunnel with 0.3 m x 0.3 m x 0.6 m test section and crossflow velocities of 0-65 m/s.

The round liquid jets were injected vertically downward using a pressure feed system as illustrated in Fig. 1. The test liquid was contained within a cylindrical test chamber having a diameter of 50 mm and a length of 100 mm, constructed of type 304 stainless steel. The nozzle was located along the axis at the bottom of the test chamber. Round supercavitating nozzles were used that had sharp edged inlets and exits yielded uniform nonturbulent round liquid jets as discussed by Wu et al.[18] and Lienhard[19]. Round nozzles with large length/diameter ratio (>40) were used to generate fully developed turbulent pipe flow at the nozzle exit.

The test liquid was placed within the test chamber using the liquid fill line (note that surface tension and vacuum created inside the chamber upon closing the fill line acted naturally to prevent premature outflow of liquid). The flow of the liquid jet was initiated by admitting pressurized air to the top of the test chamber upon activation of a solenoid valve. The pressure of the air in the test chamber was varied to provide liquid velocities at the jet exit of 10-45 m/s. The air used to pressurize the injected liquid was stored in a large (1.3 m^3 volume) air reservoir set to the desired injection pressure by filling from the laboratory high-pressure air supply system (air supply system pressures were up to 1500 kPa, with dewpoints less than 240 K). A baffle across the air inlet of the cylindrical chamber prevented excessive aeration of the test liquid by the pressuring air during liquid jet injection. Test times in the shock tube were short, however, this was not a problem because flow development times (taken as the time required for a given liquid sample to cross the test section) were smaller than 7 ms which were less than 1/3 of the available test times. In addition, data acquisition times using pulsed shadowgraphy and holography were even shorter, less than 10 ns, and did not impose any significant test time requirements. Finally, timing of the breaking of the diaphragm of the shock tube and starting the liquid jet flow was controlled so that the jet flow was present, with the liquid jet passing out of the shock tube without splashing through a hole in the bottom of the tube just opposite the nozzle location. Naturally, once the crossflow was present, deflection of the jet caused it to strike the lower inside surface of the shock tube downstream of the hole, however, this was not a problem because the crossflow swept the splashed liquid downstream away from the liquid jet so that observations of the liquid jet itself were not obscured by splashed liquid. The test time in the wind tunnel was much larger and did not cause any problem.

III. Computational Methods

The measurements of Mazallon et al.[1] and Sallam et al.[2] showed that the deformation and breakup properties of round nonturbulent liquid jets in uniform crossflows were independent of liquid jet velocities which implies that the various streamwise planes of the liquid jet do not interact. This assumption was adopted during the present computational study so that liquid column behavior was taken to be equivalent to the temporal behavior of an initially motionless two-dimensional cylindrical liquid jet element subjected to a step increase of the ambient crossflow velocity. It was further assumed that effects of evaporation are small, liquid and gas phase properties are constant, the liquid jet velocity remains constant at its initial value, V_j, and the liquid jet flow and the crossflow are nonturbulent. Notably, all these assumptions correspond to the experimental conditions of Mazallon et al.[1] and Sallam et aI.[2] Under these approximations, the distance traversed by the cylindrical jet element in the initial jet direction, y, is therefore the product of the constant jet velocity, V_j, and the time of interaction between the liquid jet and the crossflow, t:

$$y = V_j t \tag{1}$$

The time-dependent and two-dimensional Navier-Stokes equations were solved in both the gas and the liquid phases using the projection method of Chorin.[20] The discretization in space was carried out on a staggered grid according to the incompressible marker and cell (MAC) method of Harlow and Welch.[21] The liquid/gas interface was captured by the level-set method of Sussman et al.[22] This approach yielded the local fluid properties of each cell with a smooth transition between the gas and the liquid phases near the interface. A redistancing algorithm due to Sussman and Fatemi[23] was used to maintain the level-set as an accurate distance function at all times. The interface calculations allowed for effects of surface tension, pressure and shear forces, with surface tension represented by a

body force distributed over an interface having finite thickness, following Brackbill et al.[24] The discretizations in both space and time were second order accurate. When eddy shedding was absent, the domain size was 5 d_j wide and 12.5 d_j long and was covered with a moving grid that was 256-512 elements wide and 640-1280 elements long. The boundary conditions were symmetric along the sides of the computational domain with a constant fluid velocity across the inlet and a fixed pressure along the outlet. When eddy shedding was present, the domain width and the number of elements were doubled with no assumption of symmetry of the flow over the liquid jet. Tests of various sized solution regions and finer grids caused less than a 2.5% change of computational results reported in the following; therefore, computational errors are conservatively estimated to be smaller than 4%. The computational model details and other major assumptions of the analysis are detailed by Aalburg et al.[3] The ranges of present calculations were as follows: Reynolds numbers of 12.5-200, Weber numbers of 0.1-100,000, Ohnesorge numbers of 0.001-100, liquid/gas density ratios of 2-00 and liquid/gas molecular viscosity ratios of 0.001-1,000.

IV. Results and Discussion

A. Nonturbulent Liquid Jet in Crossflow

Visualizations of nonturbulent round liquid jets without crossflow and in gas crossflows within bag, multimode and shear breakup regimes are shown in Fig. 2. The test conditions are as follows We = 0, no breakup; We = 8, bag breakup; We = 30, multimode breakup; and We = 220, shear breakup. Mazallon et al.[1] and Sallam et al.[2] showed a useful general analogy between the primary surface breakup of nonturbulent round liquid jets in crossflow and the secondary breakup of drops subjected to shock wave disturbances which suggests modest streamwise interactions in the liquid jets. They found that the transitions to various breakup regimes are not influenced significantly by liquid viscosities for Oh < 0.1. Transition to bag breakup occurred at We = 5, to multimode breakup at We = 30, and to shear breakup at We = 110. They also identify conditions required for the onset of breakup and for the breakup of the entire liquid column itself and the trajectory properties of the liquid jet.

B. Shear Breakup of Nonturbulent Liquid Jet in Crossflow

Sallam et al.[2] studied the formation of ligaments and drops along the liquid jet surface for round nonturbulent liquid jets in crossflow within shear and multimode breakup regime. They identified two regimes for both the onset of ligament formation along the liquid surface and for the variation of ligament diameter as a function of distance along the liquid surface: (1) an initial transient regime associated with the growth of a shear layer near the liquid surface which supplies liquid to the base of ligaments, and (2) a quasi-steady regime where the shear layer reaches its maximum possible growth within the confines of the round liquid jet and has a thickness that is a fixed fraction of the liquid jet diameter. In both regimes of ligament growth, drops formed at the tips of ligaments were a fixed multiple of the ligament diameter; thus, this behavior generally supports drop formation at the tips of ligaments by the classical Rayleigh breakup mechanism. The ligaments and drops sizes along the liquid jet surface for nonturbulent liquid jet within the shear and multimode breakup regimes are plotted in Fig. 3. The drop velocity distributions after breakup, plotted in Fig. 4., were found to be relatively independent of drop size and approximated the liquid jet velocity, v_j, in the y direction but were somewhat larger than the characteristic liquid-phase velocity in the x direction, and were given by:

$$u_p/u_L = u_p(\rho_L/\rho_G)^{1/2}/u_\infty = 6.4 \qquad (2)$$

This is probably due to drag on the drops by the crossflowing gas as the drops are formed.

C. High Oh Nonturbulent Jet breakup in Crossflow

The computational study of Aalburg et al.[3] investigated the deformation of nonturbulent round liquid jets in crossflow for Oh of 0.001-100, and liquid/gas density ratios of 2-∞. They constructed a liquid column deformation and breakup regime map as shown in Fig. 5, plotted as $We^{1/2}/Oh$ as a function of 1/Oh, that yielded constant deformation and breakup regime boundaries at large Oh, where liquid viscous effects are important, that were relatively independent of other parameters of the flow. Thus, this deformation and breakup regime map is complementary to the classical map of Hinze[26] which yield constant transitions lines at low Oh.

The Visualization of liquid crossections as a function of time for various liquid/gas density ratios 2, 6, and 32 are shown in Fig. 6. for crossflow Re = 50, Oh = 0.01, crossflow We = 32 at dimensionless times of t/t* = 0, 1, 2, …, 6, where t* is the characteristic aerodynamic time due to Rancher and Nicholls[26]. The liquid/gas density ratio had a surprisingly small effect on the deformation and the breakup for values of $\rho_L/\rho_G > 30$, particularly when Oh is small.

The crossflow Reynolds number effects on the deformation and breakup properties of liquid jets are shown in Fig. 7. For Re > 50, the liquid jet drag coefficient is relatively independent of Reynolds number and thus the effect of the Re is small. As Re is reduced below Re = 50, the crossflow approaches the Stokes range and liquid jet resistance to deformation and breakup increases.

D. Bag Breakup of Nonturbulent Liquid Jet in Crossflow

Nonturbulent liquid jet in crossflow within bag breakup regime is characterized by column waves that involve the deflection of the entire liquid column in the streamwise direction as shown in the inset of Fig. 8. The wavelengths of the column waves were independent of the crossflow Weber number and the liquid/gas momentum ratio as shown in Fig. 8. This suggests that the disturbances were convected along the liquid column. The wavelength, λ_c, of these disturbances was taken to be the distance between nodes on the upstream side of the liquid jet as illustrated in the inset of Fig. 8. Also shown in Fig. 8 are the measurements of Mazallon et al.[1] The present measurements are in good agreement with the experimental results performed by Mazallon et al.,[1] within experimental uncertainties of less than 25% at 95% confidence level, and are represented by:

$$\lambda_c / d_j = 2.7 \tag{3}$$

Notice that the correlation given by Mazallon et al.[1] was valid for the three-breakup regimes; column breakup regime, bag breakup regime, and multimode breakup regime.

Another feature of the bag breakup of nonturbulent liquid jets in crossflow that was first observed during the present investigation is the downwind surface waves shown in Fig. 9. To observe these waves the camera was tilted 40 degrees in the downwind direction from the normal position to the crossflow, as shown in the inset of Fig. 9. The downwind surface waves occur in the vicinity of the sides of the liquid column towards the downwind direction. Their temporal and spatial characterization is currently investigated.

The sizes of liquid drops resulting from the breakup of the bag membrane were independent of the crossflow Weber number as shown in Fig. 10 and are represented by:

$$SMD_{Bag} / dj = 0.15 \tag{4}$$

This is could be attributed to the fact that the bag membrane must attain certain thickness before breaking up, resulting in monodisperse spray.

E. Breakup of Turbulent Liquid Jets in Crossflow

The effect of liquid jet turbulence on the breakup regimes is illustrated in Fig. 11. The images (a) – (e) are for turbulent liquid jets at a crossflow Weber number of 16 and a jet Reynolds number of Re_{fd} = 3420, 19000, 40000, 90000 and 140000, respectively. Test liquid in image (a) is glycerol (44 % glycerin by mass). Test liquid in images (b), (d), and (e) is water and the test liquid in image (c) is ethanol. The liquid jet velocities for images (a) – (e) are 8.2 m/s, 8.2 m/s, 29.0 m/s, 38.4 m/s and 59.5 m/s, respectively. The crossflow velocities are 21.5 m/s for water, 20.9 m/s for glycerol and 13.3 m/s for ethanol. As seen in the images (a) and (b), bags are formed at crossflow Weber number of 16 and liquid jet Reynolds number ranges from 3420 to 19200 similar to those associated with nonturbulent liquid jets n crossflow. In images (c), (d) and (e), however, when the liquid jet Reynolds number is increased whereas the crossflow Weber number is kept constant, no bags were observed. Instead the liquid jet surface becomes irregular and the irregularities increase with increasing distance from the jet exit and finally form ligaments and drops. This is typical of turbulent primary breakup mechanism. Another difference is that in images (a) and (b), the liquid column diameter starts to decrease slightly with increasing distance from the jet exit whereas in images (c), (d), and (e) the liquid jet spreads radially causing an increase in the jet column diameter, typical of turbulent jets at high Reynolds number. Another important feature is that no ligaments are formed on the upwind side for the turbulent jets in images (a) and (b), unlike the turbulent liquid jets in images (c), (d) and (e). These features are attributed to the interaction of the turbulent eddies within the liquid jet with the jet free surface. At high liquid jet Reynolds numbers, these turbulent eddies would have enough kinetic energy to cause surface breakup not only at the downwind side, but also at the upwind side, despite the presence of the gaseous crossflow. This breakup mode will be called turbulent breakup. An increase in the crossflow velocity, however, expressed as a decrease in the liquid/gas momentum ratio, would suppress the upwind surface breakup. This occurs because the energy of turbulent eddies in the liquid jet is not large enough to overcome the combination of liquid surface tension forces and the pressure forces exerted by the gaseous crossflow. This breakup mode, where drops are formed only on the downwind side will be called aerodynamic breakup. The breakup regime map for turbulent jets in crossflow is

shown in Fig. 12. In this map, liquid jet Reynolds number, Re_{Ld} is plotted on the x-axis and the dimensionless quantity $We_{L\Lambda}q^{1/3}$ is plotted on the y-axis. The correlation that best describes the transition from aerodynamic breakup to turbulent breakup is as follows:

$$We_{L\Lambda}q^{1/3} = 17{,}000 \tag{5}$$

It is observed that both turbulent and aerodynamic breakup occurs for the range of Reynolds numbers, Re_{Ld} = 6,000 – 60,000, with the transition controlled mainly by $We_{L\Lambda}q^{1/3}$. The authors would like to call this new dimensionless number as the Faeth Number (Fa) to honor the memory of Prof. Faeth.

The measurements of SMD after turbulent primary breakup along the surface of turbulent round liquid jets in still and crossflowing gases were obtained by Lee et al.[4] and are plotted in Fig. 13, along with earlier measurements of drop sizes after turbulent primary breakup in still gases due to Wu and Faeth.[27] The agreement between the results of Wu and Faeth[25] and the present investigation is excellent and yields the following combined correlation:

$$SMD/\Lambda = 0.56\,[y/(\Lambda We_{L\Lambda}^{1/2})]^{0.5} \tag{6}$$

Finally, mean streamwise and cross stream drop velocities after turbulent primary breakup were measured by Lee et al.[4] for both still and crossflowing environments. These measurements were obtained close to the tips of ligaments in order to minimize effects of drop velocity relaxation to the ambient velocity. The resulting drop velocity distributions in the streamwise direction, v_p, and in the cross stream direction, u_p, are illustrated in Fig. 14. Streamwise velocities are plotted for turbulent round liquid jets in both still and crossflowing air while cross stream velocities are plotted only for turbulent round liquid jets in crossflowing air. The drop velocity distributions are uniform and nearly independent of the drop diameter. The velocity correlations of the measurements illustrated in Fig. 14 follow the normalizations by Sallam et al.[2] for drop velocities after primary breakup from nonturbulent round liquid jets in crossflows:

$$v_p / v_j = 0.75 \tag{7}$$

$$u_p / u_L = u_p / [(\rho_G / \rho_L)^{1/2} u_\infty] = 4.82 \tag{8}$$

These results indicates drag effects of the gas phase on the drop velocities after breakup, that tend to reduce streamwise drop velocities from the streamwise jet velocity and to increase cross stream drop velocities significantly from the characteristic cross stream velocity.

V. Conclusions

The liquid jet deformation and the formation of ligaments and drops, as well as the extent of the entire liquid column, were studied experimentally and computationally for liquid jets in air crossflows at normal temperature and pressure. The major conclusions of the study were as follows:

1) At small Ohnesorge numbers, Oh<<1, the breakup of laminar round liquid jets in crossflows is mainly a function of the Weber number, whereas at large Ohnesorge numbers, Oh>>1, it is mainly a function of $We^{1/2}/Oh$.
2) At small liquid/gas density ratios the resistance of laminar round liquid jets in crossflows to breakup progressively increases due to increasing relaxation of the jet towards the crossflow velocity during deformation and breakup. At small Reynolds numbers (Re<10) the resistance of laminar round liquid jets in crossflows to breakup progressively increases due to increasing drag forces and associated increasing relaxation of the jet towards the crossflow velocity during deformation and breakup.
3) For nonturbulent liquid jet in crossflow within the shear breakup regime the drop velocity distributions after breakup were relatively independent of drop size. The Ligament diameters along the liquid surface increases with increasing distance in the y direction for a time before reaching a steady condition and became relatively independent of distance from the jet exit. The drop sizes were comparable to the size of the ligaments.
4) For nonturbulent liquid jet in crossflow within the bag breakup regime the column waves were independent of the crossflow Weber number and the liquid/gas momentum ratio. New downwind surface waves were observed to occur in the vicinity of the sides of the liquid column towards the downwind direction. The drop sizes resulting from the breakup of the bag membrane were independent of the crossflow Weber number.

5) The Breakup of turbulent liquid jet in crossflow falls into two major regimes known as aerodynamic breakup regime and turbulent breakup regime, separated by a new dimensionless parameter (Faeth number) $Fa = We_{LA}q^{1/3} = 17{,}000$. Aerodynamic breakup regimes of turbulent liquid jets ($Fa < 17{,}000$) included column, bag, multimode and shear, similar to the non turbulent liquid jets in gaseous crossflow.

Acknowledgments

The authors dedicate the present paper to the memory of Prof. Gerard M. Faeth. Prof. Faeth was the Ph.D. advisor and mentor of the first, fourth and fifth authors. It has been their honor and privilege to be his students. The work at Oklahoma State University was supported by the National Science Foundation under Grant No. EPS-0132534 (Oklahoma - EPSCoR). The work at the University of Michigan was sponsored by the Air Force Office of Scientific Research, Grant No. F49620-02-1-0007, under the technical management of J.M. Tishkoff. Assistance from undergraduate students: Richa Jolly and Diana Ma at the University of Michigan, and Morgan Wright and Sam Parker at Oklahoma State University is greatly appreciated. The U.S. Government is authorized to make copies of this article for governmental purposes notwithstanding any copyright notation thereon.

References

[1]Mazallon, J., Dai, Z., and Faeth, G.M., "Primary Breakup of Nonturbulent Round Liquid Jets in Gas Crossflows," *Atomization and Sprays*, Vol. 9, No. 3, 1999, pp. 291-311.

[2]Sallam, K.A., Aalburg, C., and Faeth, G.M., "Breakup of Round Nonturbulent Liquid Jets in Gaseous Crossflow," AIAA Journal, Vol. 42, No. 12, 2004, pp. 2529-2540.

[3]Aalburg, C., Van Leer, B., Faeth, G.M., and Sallam, K.A., "Properties of Nonturbulent Round Liquid Jets in Uniform Gaseous Crossflows," Atomization and Sprays, Vol. 15 No. 3, 2005, pp. 271-294.

[4]Lee, K., Aalburg, C., Diez, F. J., Faeth, G.M., and Sallam, K.A., "Primary Breakup of Turbulent Round Liquid Jets in Uniform Crossflows," AIAA J., Submitted.

[5]Wu, P.-K., Kirkendall, K.A., Fuller, R.F., and Nejad, A.S., "Breakup Processes of Liquid Jets in Subsonic Crossflows," *Journal of Propulsion and Power*, Vol. 13, No. 1, 1997, pp. 64-73.

[6]Geary, E.L., and Margettes, M.J., "Penetration of a High Velocity Gas Stream by a Water Jet," *Journal of Spacecraft*, Vol. 6, No. 1, 1969, pp. 79-81.

[7]Reichenbach, P.R., and Horn, K.P., "Investigation of Injectant Properties in Jet Penetration in a Supersonic Stream," *AIAA Journal*, Vol. 9, No. 3, 1971, pp. 469-471.

[8]Kush, E.A., and Schetz, J.A., "Liquid Jet Injection into a Supersonic Flow," *AIAA Journal*, Vol. 11, No. 9, 1979, pp. 1223-1224.

[9]Schetz, J.A., and Paddye, A., "Penetration of a Liquid Jet in Subsonic Airstreams," *AIAA Journal*, Vol. 15, No. 10, 1977, pp. 1385-1390.

[10]Schetz, J.A., Kush, E.A., and Joshi, P.B., "Wave Phenomena in Liquid Jet Breakup in a Supersonic Crossflow," *AIAA Journal*, Vol. 15, 1979, pp. 774-778.

[11]Nejad, A.S., and Schetz, J.A., "Effects of Properties and Location in the Plume on Droplet Diameter for Injection in a Supersonic Stream," *AIAA Journal*, Vol. 21, No. 7, 1983, pp. 956-961.

[12]Nejad, A.S., and Schetz, J.A., "Effects of Viscosity and Surface Tension on a Jet Plume in Supersonic Cross-Flow," *AIAA Journal*, Vol. 22, No. 4, 1984, pp. 458-459.

[13]Less, D.M., and Schetz, J.A., "Transient Behavior of Liquid Jets Injected Normal to a High-Velocity Gas Stream," *AIAA Journal*, Vol. 24, No. 12, 1986, pp. 1979-1985.

[14]Kitamura, Y., and Takahashi, T., "Stability of a Liquid Jet in Air Flow Normal to the Jet Axis," *Journal of Chemical Engineering of Japan*, Vol. 9, No. 4, 1976, pp. 282-286.

[15]Nguyen, T.T., and Karagozian, A.R., "Liquid Fuel Jet in a Subsonic Crossflow," *Journal of Propulsion and Power,* Vol. 8, No. 1, 1992, pp. 21-29.

[16]Karagozian, A.R., "An Analytical Model for the Vorticity Associated with a Transverse Jet," *AIAA Journal*, Vol. 24, 1986, pp. 429-436.

[17]Higuera, F.J., and Martinez, M., "An Incompressible Jet in a Weak Crossflow," *Journal of Fluid Mechanics*, Vol. 249, 1993, pp. 73-97.

[18]Wu, P.-K., Miranda, R.F., and Faeth, G.M., "Effects of Initial Flow Conditions on Primary Breakup of Nonturbulent and Turbulent Round Liquid Jets." *Atomization and Sprays*, Vol. 5, 1995, pp. 175-196.

[19]Lienhard, J.H., "Velocity Coefficients for Free Jets from Sharp-Edged Orifices," *Journal of Fluids Engineering*, Vol. 106, 1984, pp. 13-17.

[20]Chorin, A.J., "Numerical Solution of the Navier-Stokes Equations," Mathematics of Computation, Vol. 22, No. 104, 1968, pp. 745-762.

[21]Harlow, F.H., and Welch, J.E., "Numerical Calculation of Time-Dependent Viscous Incompressible Flow of Fluid with Free Surface," Phys. Fluids, Vol. 8, No. 12, 1965, pp.2182-2189.

[22]Sussman, M., Smereka, P., and Osher, S., "A Level Set Approach for Computing Solutions to Incompressible Two-Phase Flow," J. Comp. Phys., Vol. 114, No. 1, 1994, pp. 146-159.
[23]Sussman, M., and Fatemi, E., "An Efficient, Interface Preserving Level Set Redistancing Algorithm and its Application to Interfacial Incompressible Flow," SIAM J. Sci. Computing, Vol. 20, No.4, 1999, pp. 1165-1191.
[24]Brackbill, J.U., Kothe, D.B., Zemach, C., "A Continuum Method for Measuring Surface Tension," J. Comp. Phys., Vol. 100, 1991, pp. 335-354.
[25]Hinze, J.O., "Fundamentals of the Hydrodynamic Mechanism of Splitting in Dispersion Processes," *AIChE Journal*, Vol. 1, No. 3, 1955, pp. 289-295.
[26]Ranger, A.A., and Nicholls, J.A., "The Aerodynamic Shattering of Liquid Drops," *AIAA Journal*, Vol. 7, No. 2, 1969, pp. 285-290.
[27]Wu, P.-K., and Faeth, G.M., "Aerodynamic Effects on Primary Breakup of Turbulent Liquids," Atomization and Sprays, Vol. 3, No. 3, 1993, pp. 265-289.

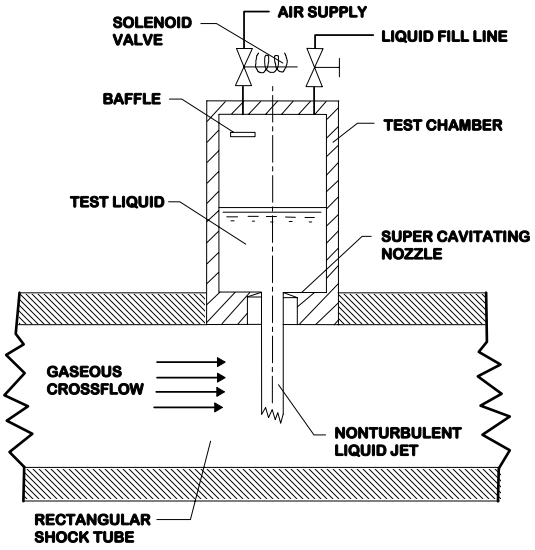

Figure 1. Sketch of the test apparatus.

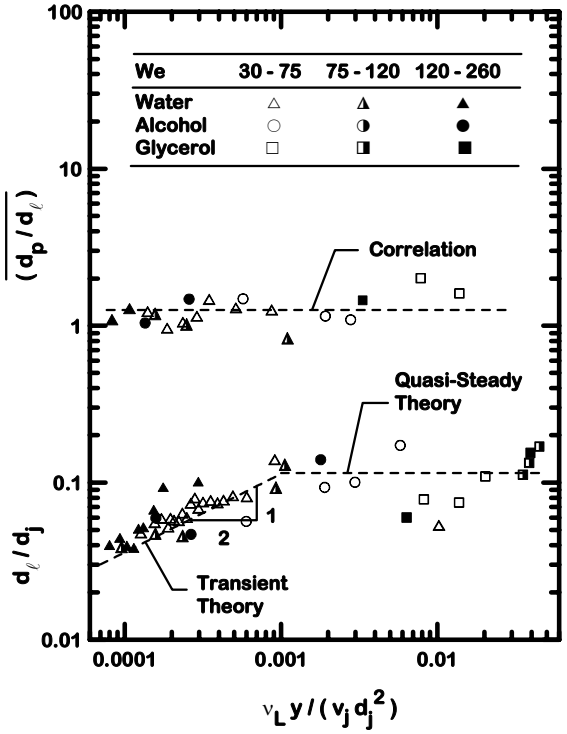

Figure 3. Diameters of ligaments and drops as a function of time of jet flow (height) during primary breakup of nonturbulent round liquid jets in air crossflows.

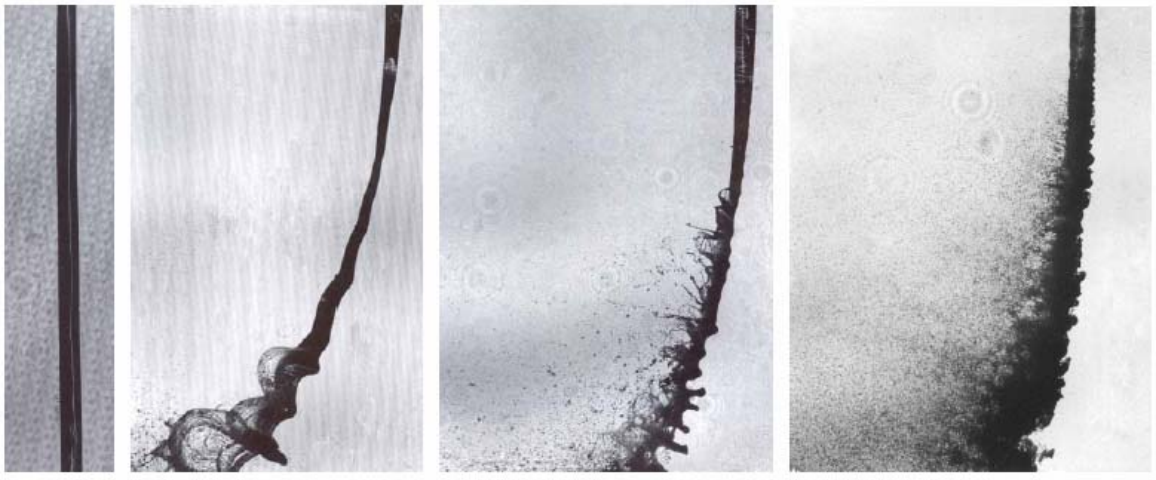

Figure 2. Visualizations of nonturbulent round liquid jets in gas crossflows: We = 0, no breakup; We = 8, bag breakup; We = 30, multimode breakup; and We = 220, shear breakup.

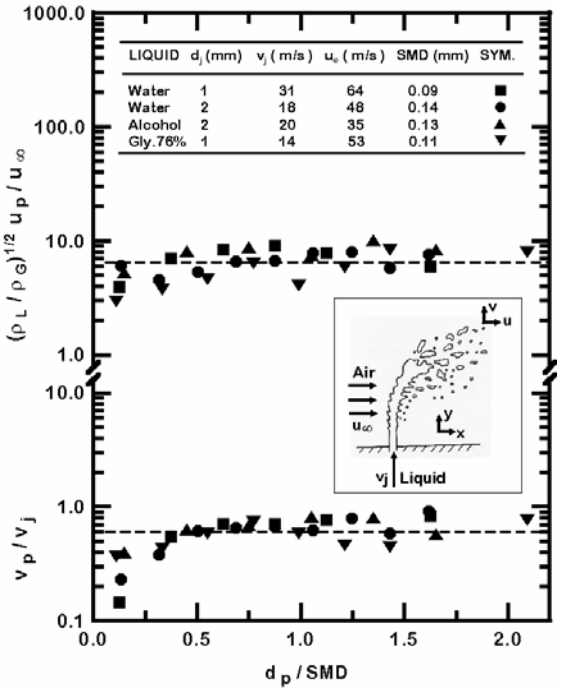

Figure 4. Streamwise and crosstream drop velocity distributions after primary breakup of nonturbulent round liquid jets in air crossflows.

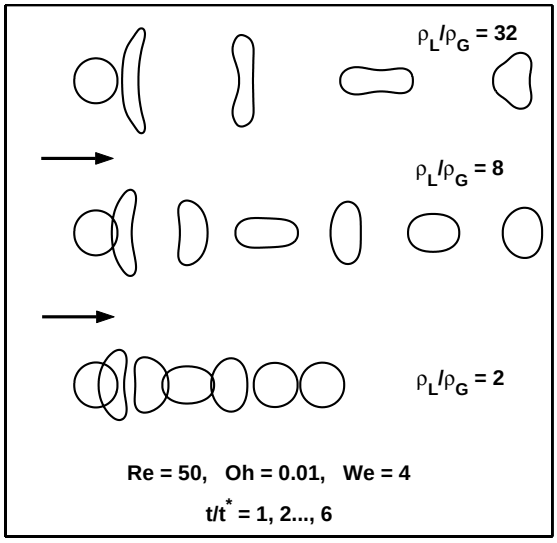

Figure 6. Visualization of liquid crossections as a function of time for various liquid/gas density ratios (Re = 50, Oh = 0.01, We = 32, t/t* = 0, 1, 2, …, 6).

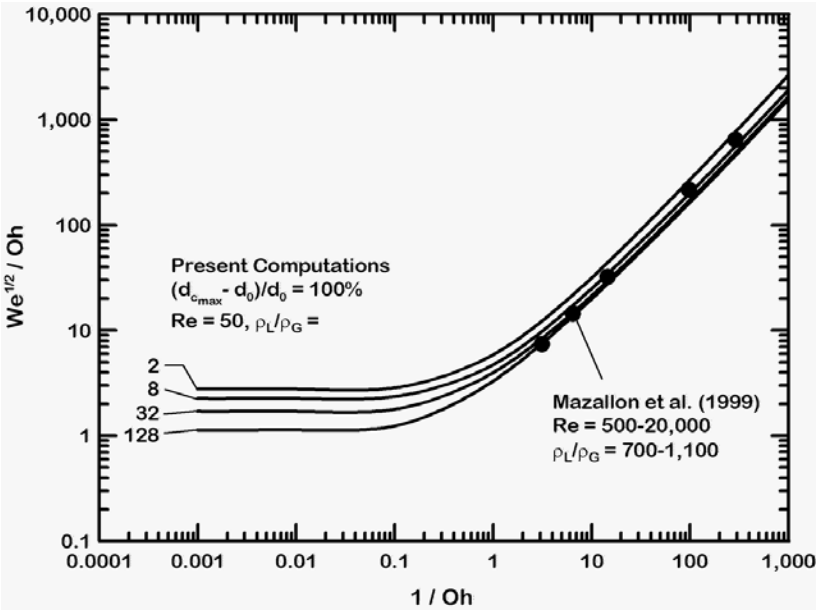

Figure 5. Predicted and measured liquid jet breakup regime map in drag-force/liquid-viscous-force ($We^{1/2}$/Oh) and surface-tension-force/liquid viscous force (1/Oh) coordinates.

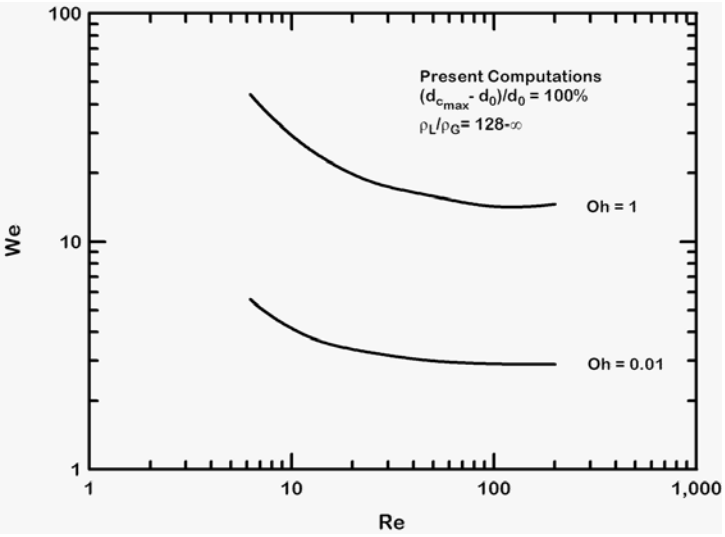

Figure 7. Effects of crossflow Reynolds number on the Weber number required for 100% deformation of liquid jets for various Ohnesorge number.

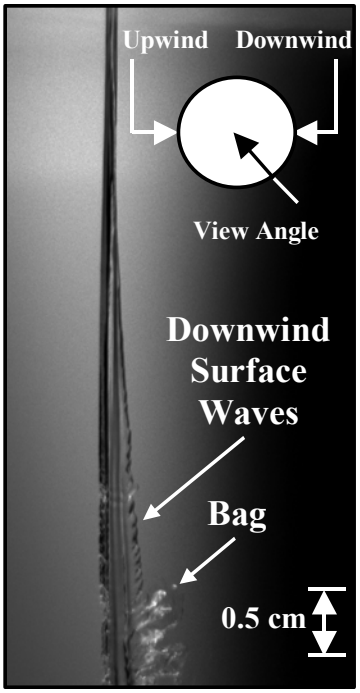

Figure 9. Downwind surface waves of round nonturbulent liquid jets in uniform gaseous crossflow within the bag breakup regime. Water, d_j = 1 mm, We_G = 24, and q = 1199.

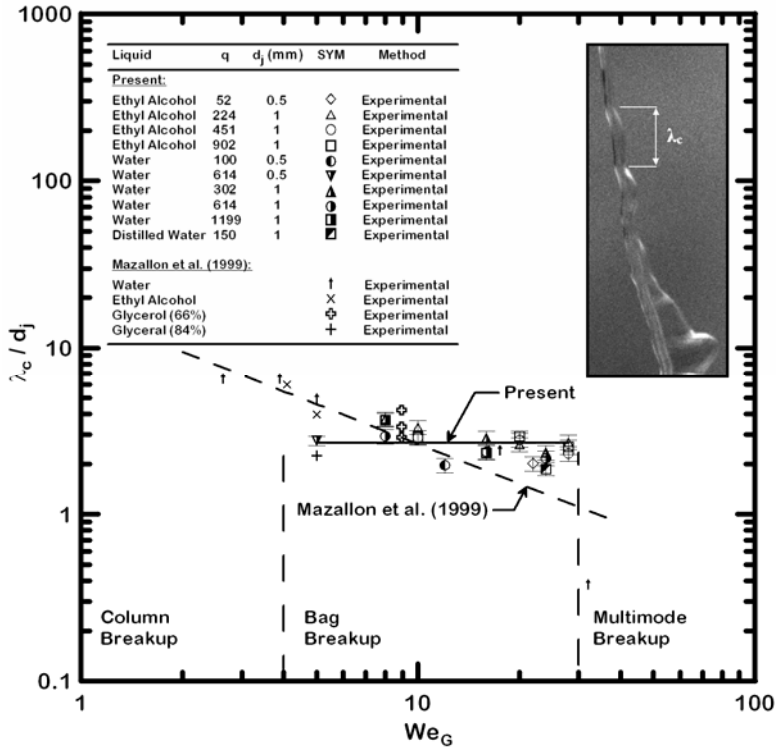

Figure 8. Liquid column wavelengths as a function of Weber number.

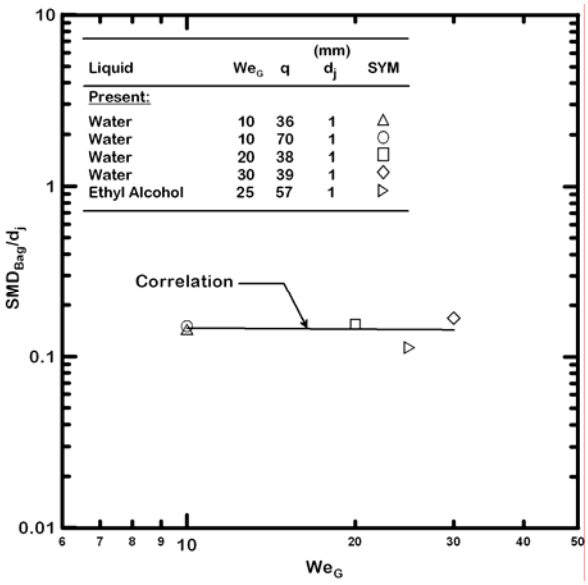

Figure 10. Liquid droplets size due to bag breakup of round nonturbulent liquid jets in uniform gaseous crossflow.

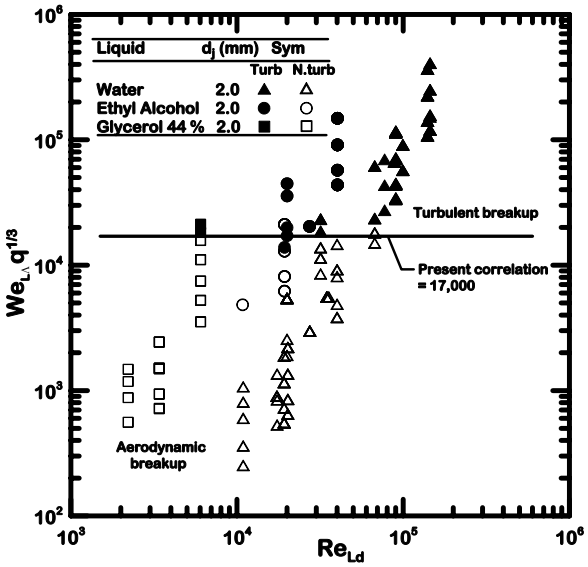

Figure 12. Breakup regime map showing transition between turbulent breakup and aerodynamic breakup.

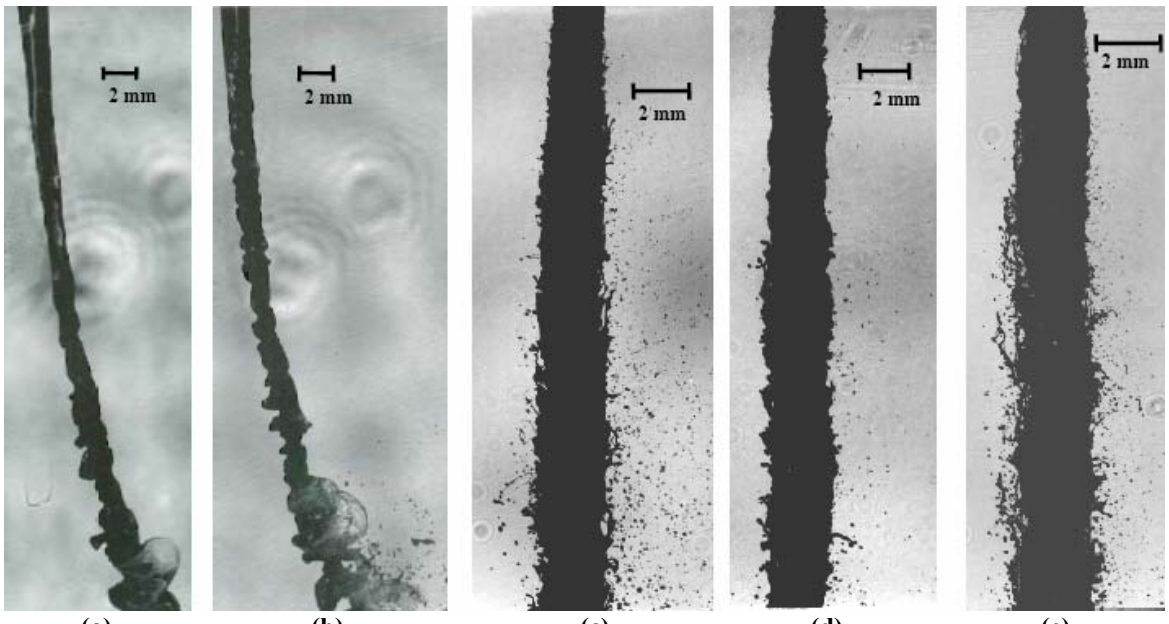

Figure 11. Flow visualizations showing effect of Reynolds number on bag breakup regimes. We_∞ = 16, d_j = 2.0 mm. (a) Glycerol, Re_{Ld} = 3,420, v_j = 8.2 m/s, u_∞ = 20.9 m/s, (b) Water, Re_{Ld} = 19,000, v_j = 8.2 m/s, u_∞ = 21.5 m/s (c) Ethanol, Re_{Ld} = 40,000, v_j = 29.0 m/s, u_∞ = 13.3 m/s (d) Water, Re_{Ld} = 90,000, v_j = 38.4 m/s, u_∞ = 21.5 m/s (e) Water, Re_{Ld} = 140,000, v_j = 59.5 m/s, u_∞ = 21.5 m/s. The crossflow is from left to right in all images.

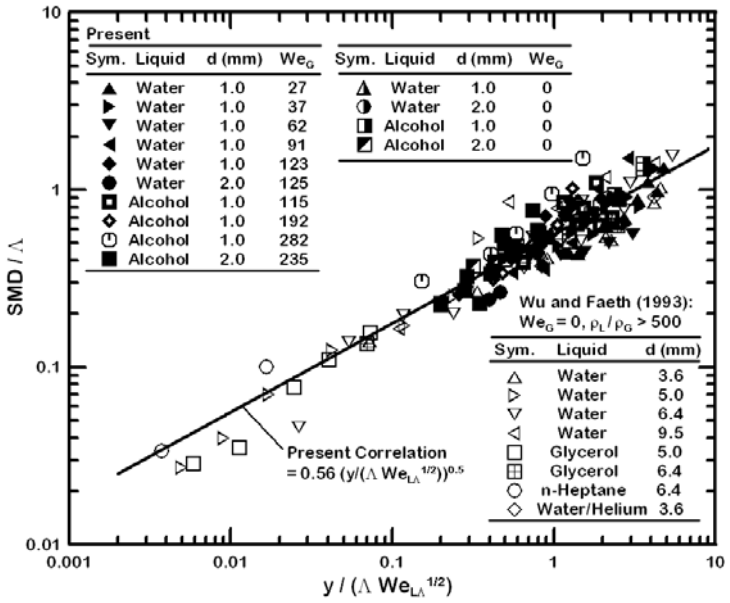

Figure 13. Drop diameters after primary breakup for turbulent round jets in still air and in cross flow as a function of normalized

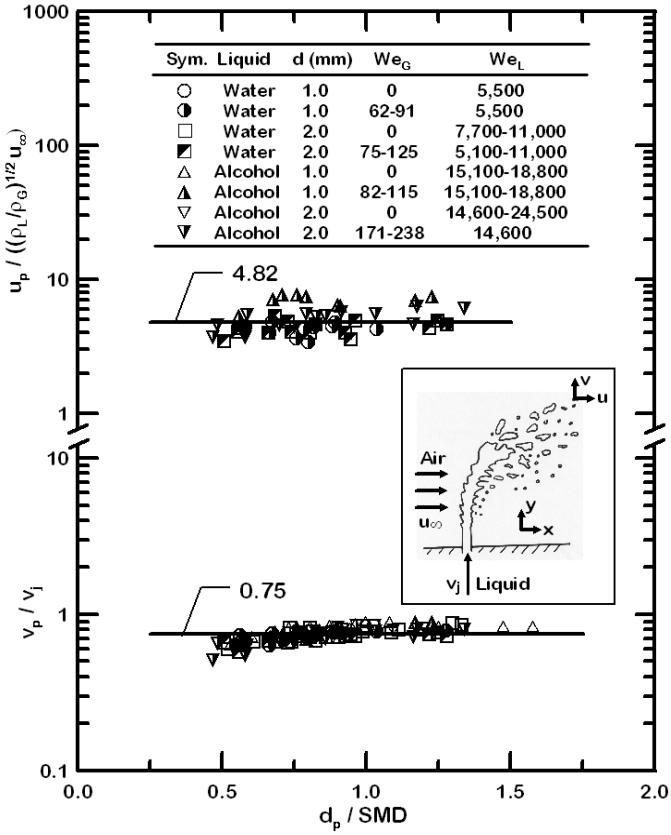

Figure 14. Streamwise and cross stream drop velocities after breakup as function of drop sizes for turbulent round liquid jet in crossflow.